Online Repository

METHODS

Mice

CCR10-knockout (KO)/EGFP-knockin (KI) mice were previously generated in our lab [E1]. In heterozygous $CCR10^{+/EGFP}$ (or $CCR10^{+/-}$) mice, one copy of the CCR10 coding sequence of the genome was replaced with a coding sequence for EGFP (enhanced green fluorescent protein) and another copy of wild-type CCR10 allele remains, while in homozygous $CCR10^{EGFP/EGFP}$ (or $CCR10^{-/-}$) mice, both copies of the CCR10 coding sequences were replaced with EGFP coding sequences [E1]. In experiments, $CCR10^{+/EGFP}$ mice were used to substitute for wild-type $CCR10^{+/+}$ mice as controls so that we could use EGFP as a reporter for the CCR10 expression. $Rag1^{-/-}$ mice were purchased from Jackson lab. $CCR10^{-/-}Rag1^{-/-}$ and $CCR10^{+/-}Rag1^{-/-}$ mice were generated through crossing CCR10-KO/EGFP-KI mice and $Rag1^{-/-}$ mice. All mice were on the C57BL/6 genetic background. Sex-matched male and female adult littermate mice (8-12 weeks) were used in experiments. All mouse experiments were performed in specific pathogen-free conditions in accordance with protocols approved by Institutional Animal Care and Use Committees of The Pennsylvania State University and University of Texas Health Science Center at San Antonio.

Antibodies and Reagents

All antibodies used are against mouse antigens. Alexa Fluor 700-conjugated anti-CD45 (30-F11), Phycoerythrin (PE)-Cy7-conjugated anti-TCRβ (H57-597), Allophycocyanin (APC)- or APC-Cy7-conjugated anti-IL-17A (TC11-18H10.1), APC-or PE-Cy7-conjugated IFNγ (XMG1.2), Alexa Fluor 647-conjugated anti-CD4 (GK1.5), and PE-Cy7-conjugated anti-TCRδ (GL3) antibodies were purchased from Biolegend. BV421-conjugated anti-CD3 (145-2C11) antibody was purchased from BD Bioscience. APC-conjugated anti-IL-22 (IL22JOP) antibody was purchased from eBioscience. The 'cocktail' of antibodies to lineage markers (CD5, B220, CD11b, Gr-1, 7-4 and Ter-119) were from Miltenyi Biotec (catalog number: 130-092-613). Aldara cream containing 5% imiquimod (IMQ) was purchased from a local pharmacy. Mouse CCL27 was purchased from PeproTech.

Fabrication of microneedle patches

Microneedle patches were fabricated as we recently described [E2]. In brief, to fabricate one microneedle patch, a solution of polyvinylpyrrolidone (PVP) and polyvinyl alcohol (PVA) (25% w/v) containing CCL27 proteins (2 μg) was cast onto the polydimethylsiloxane mold and forced into the microneedle cavities by vacuum and centrifugation. After the microneedles were solidified, another PVP/PVA (50 % w/v) solution was cast on the top of the microneedle array as a base plate to form the final microneedle patch. Each microneedle patch consisted of 100 (10 × 10) pyramidal microneedles with a height, base and tip-to-tip distance of 600, 200 and 500 μm respectively. The microneedle patch was peeled off the mold and stored at 4^{o}C until use.

Reconstitution of $Rag1^{-/-}$ mice with $CD4^{+}$ αβT cells

Purified splenic $CD4^{+}$ αβT cells were transferred into recipient mice through intravenous injection as described [E3]. $CD4^{+}$ T Cell Isolation Kit (Miltenyi biotec, Cat #: 130-104-454) was used to isolate $CD4^{+}$ αβT cells. Briefly, splenic cells of $CCR10^{+/-}$ or $CCR10^{-/-}$ donor mice were stained with a $CD4^{+}$ T Cell biotin-antibody cocktail, followed with anti-biotin MicroBeads. The

stained cells were applied to a magnetic-activated cell-sorting (MACS) column to isolate $CD4^+$ αβT cells. The purity of isolated CD4+ αβT cells is > 97%. One million cells were transferred to one $Rag1^{-/-}$ mouse. Eight weeks after the transfer, recipients were used in imiquimod-induced skin inflammation experiments.

Induction of skin inflammation with topical application of imiquimod

The experiment was performed similarly as described [E4]. Briefly, the back of mice was removed of hair and topically applied with a daily dose of Aldara cream containing 3.125 mg of imiquimod. Different days after starting the IMQ application, mice were euthanized and analyzed.

Treatment of imiquimod-induced skin inflammation with microneedle-mediated transdermal delivery of CCL27

CCL27-loaded or empty microneedle patches were applied onto the IMQ-treated skin using a spring-loaded applicator (Micropoint Technologies Pte., Ltd. Singapore). One patch composed of 100 (10 X10) microneedles is loaded with total 2 μg CCL27 proteins and covers a 0.5 cm X 0.5 cm area. After microneedles were inserted into the skin, the base of the microneedle patch was fixed on the skin surface with an adhesive tape for 30 min to allow the microneedle tips dissolve into the skin and then the base was removed. Different days after starting the IMQ application and CCL27 treatment, mice were euthanized and analyzed.

Cell isolation and flow cytometric analysis

Isolation of lymphocytes from the skin and flow cytometric analysis were performed as we previously described [E3].

Real-time quantitative RT-PCR

The experiment was performed as previously described [E5]. Primers for CCL27 were 5'-CCTCCCGCTGTTACTGTTG (forward) and 5'- CTTGGCGTTCTAACCACCGA (reverse).

H&E staining of skin sections and measurement of epidermal thickness

The paraffin embedding, sectioning and H&E staining of the skin were performed by the Animal Diagnostic Laboratory of the Pennsylvania State University or in house. The thickness of epidermal layers of the skin sections was measured by the software Image J.

Statistical analyses

It was assumed that sampling was from a normally distributed population. Statistical significance was determined by student T tests or one-way analysis of variance (ANOVA) followed by the Student-Newman-Keuls test. $P<0.05$ is considered significant.

DISCUSSION

Our finding that the CCL27/CCR10 axis plays an important role in restricting IL-17A/IL-22-producing skin T cell activation and inflammation in mouse models of psoriasis suggests that impairment of this axis in human patients of psoriasis contributes to progression of the disease. This finding is consistent with the clinical observation that CCL27 is severely suppressed in psoriatic lesional skin in human patients [E6, E7, E8, E9]. Since CCL27 is downregulated only in the lesional but not non-lesional skin of psoriatic patients [E6, E7, E9], impairment of the CCL27/CCR10

axis is likely involved in progression but not initiation of psoriasis. CCL27 is suppressed in the lesional skin of psoriasis but not other skin diseases such as atopic dermatitis [E7, E8], suggesting differential involvement of the axis in different skin inflammatory diseases.

Considering CCL27 is the only known ligand for CCR10 [E10], its psoriasis-associated suppression likely results in dysregulated localization and function of $CCR10^+$ skin T cells and ILCs. As in mice, a significant fraction of T cells in the normal skin of humans express CCR10 [E11, E12]. In addition, T cells migrating out of the human skin do not express CCR10 [E13], while $CCR10^+$ T cells of human blood respond to chemoattraction of CCL27 [E14, E15]. These previous findings are consistent with a role of the CCR10/CCL27 axis in localization of homeostatic T cells into the healthy skin. However, how the composition and function of $CCR10^+$ T cells changed in the psoriatic skin were not well studied. While an early report suggested that there were increased $CCR10^+$ T cells in the psoriatic skin based on immunohistochemical staining [E16], a later report found that CCR10 is reduced in the psoriatic skin based on the transcription study [E7]. Like T cells, most ILCs in the healthy skin of humans express CCR10 [E17] and a recent report also identified a population of skin-homing $CCR10^+$ ILCs in human blood [E18]. However, there is no study of $CCR10^+$ ILCs in the psoriatic skin of patients. It is not clear how function of $CCR10^+$ T cells and ILCs are altered in the psoriatic skin where expression of CCL27 is suppressed. How impairment of the CCL27/CCR10 axis is associated with dysregulated T cells and ILCs and tissue inflammation in human psoriatic skin needs further study.

Our study using mouse models here suggest that the CCL27/CCR10 axis has broad effects on preventing psoriatic inflammation through acting on various skin T cells and ILCs. We found that CCR10 expressed on skin γδT cells, αβT cells and ILCs is all involved in helping restrict skin inflammation in the IMQ-induced model of psoriasis. However, detailed molecular mechanisms could vary for the different populations of skin T cells and ILCs. We found that activated $IL\text{-}17A^+IL\text{-}22^+$ γδT cells and particularly αβT cells have downregulated expression of CCR10 in the IMQ-inflamed skin and that there is more significantly increased expansion of the $EGFP(CCR10)^{low/-}$ $IL\text{-}17A^+IL\text{-}22^+$ skin γδT and αβT cells in IMQ-treated $CCR10^{-/-}$ mice than of $CCR10^{+/-}$ mice. These results indicate that loss of CCR10-derived signals lead to increased activation of the $EGFP(CCR10)^{low/-}$ $IL\text{-}17A^+IL\text{-}22^+$ γδT17 and Th17 cells, suggesting that the CCL27/CCR10 axis not only directs localization of $CCR10^+$ T cells into the healthy skin but also restricts their activation in psoriasis. Signal pathways mediating the CCL27/CCR10 suppression of γδT17 and Th17 cell activation are unknown. However, it is known that some members of the G protein-coupled receptor family, to which CCR10 belongs to, could inhibit cellular activation through both G-protein-dependent and independent signal pathways [E19, E20]. CCR10 also could help establishment of regulatory T (Treg) cells in the skin [E11]. However, the role of Treg cells in restricting activation of γδT17 and Th17 cells is minor and they primarily restrain type 1 interferon–induced $CD8^+$ T cell responses in the IMQ-induced psoriasis [E21]. Detailed molecular mechanisms underlying the CCL27/CCR10-mediated suppression of pathogenic $IL\text{-}17A^+IL\text{-}22^+$ T cell activation remain to be determined. On the other hand, CCR10-KO does not lead to enhanced activation of $IL\text{-}17^+$ ILCs. Instead, CCR10 is required for maintenance of $CCR10^+$ skin ILCs, which have a regulatory role in suppressing activation of $IL\text{-}17A^+IL\text{-}22^+$ Th17 cells in IMQ-inflamed skin. $CCR10^+$ ILCs express high levels of MHCII and the co-inhibitory molecule PD-L1 [E3], suggesting that they could potentially function as regulatory antigen-presenting cells to regulate the T activation. Additional studies are needed to resolve molecular mechanisms

mediating the regulatory effect of $CCR10^+$ ILCs. Genetic backgrounds also influence IMQ-induced skin inflammation [E22]. It will be interesting to test whether the CCL27/CCR10 axis has same suppressive effects on the skin inflammation on different strains of mice.

REFERENCES

E1. Jin Y, Xia M, Sun A, Saylor CM, Xiong N. CCR10 is important for the development of skin-specific gammadeltaT cells by regulating their migration and location. J Immunol. 2010;185(10):5723-31.

E2. Coyne J, Davis B, Kauffman D, Zhao N, Wang Y. Polymer Microneedle Mediated Local Aptamer Delivery for Blocking the Function of Vascular Endothelial Growth Factor. ACS Biomater Sci Eng. 2017;3(12):3395-403.

E3. Yang J, Hu S, Zhao L, Kaplan DH, Perdew GH, Xiong N. Selective programming of CCR10(+) innate lymphoid cells in skin-draining lymph nodes for cutaneous homeostatic regulation. Nat Immunol. 2016;17(1):48-56.

E4. van der Fits L, Mourits S, Voerman JS, Kant M, Boon L, Laman JD, et al. Imiquimod-induced psoriasis-like skin inflammation in mice is mediated via the IL-23/IL-17 axis. J Immunol. 2009;182(9):5836-45.

E5. Hu S, Xiong N. Programmed downregulation of CCR6 is important for establishment of epidermal gammadeltaT cells by regulating their thymic egress and epidermal location. J Immunol. 2013;190(7):3267-75.

E6. Gudjonsson JE, Ding J, Johnston A, Tejasvi T, Guzman AM, Nair RP, et al. Assessment of the psoriatic transcriptome in a large sample: additional regulated genes and comparisons with in vitro models. J Invest Dermatol. 2010;130(7):1829-40.

E7. Riis JL, Johansen C, Vestergaard C, Bech R, Kragballe K, Iversen L. Kinetics and differential expression of the skin-related chemokines CCL27 and CCL17 in psoriasis, atopic dermatitis and allergic contact dermatitis. Exp Dermatol. 2011;20(10):789-94.

E8. Quaranta M, Knapp B, Garzorz N, Mattii M, Pullabhatla V, Pennino D, et al. Intraindividual genome expression analysis reveals a specific molecular signature of psoriasis and eczema. Sci Transl Med. 2014;6(244):244ra90.

E9. Sahmatova L, Sugis E, Sunina M, Hermann H, Prans E, Pihlap M, et al. Signs of innate immune activation and premature immunosenescence in psoriasis patients. Sci Rep. 2017;7(1):7553.

E10. Xiong N, Fu Y, Hu S, Xia M, Yang J. CCR10 and its ligands in regulation of epithelial immunity and diseases. Protein Cell. 2012;3(8):571-80.

E11. Xia M, Hu S, Fu Y, Jin W, Yi Q, Matsui Y, et al. CCR10 regulates balanced maintenance and function of resident regulatory and effector T cells to promote immune homeostasis in the skin. J Allergy Clin Immunol. 2014;134(3):634-44 e10.

E12. Salimi M, Subramaniam S, Selvakumar T, Wang X, Zemenides S, Johnson D, et al. Enhanced isolation of lymphoid cells from human skin. Clin Exp Dermatol. 2016;41(5):552-6.

E13. McCully ML, Ladell K, Hakobyan S, Mansel RE, Price DA, Moser B. Epidermis instructs skin homing receptor expression in human T cells. Blood. 2012;120(23):4591-8.

E14. Hudak S, Hagen M, Liu Y, Catron D, Oldham E, McEvoy LM, et al. Immune surveillance and effector functions of CCR10(+) skin homing T cells. J Immunol. 2002;169(3):1189-96.

E15. Soler D, Humphreys TL, Spinola SM, Campbell JJ. CCR4 versus CCR10 in human cutaneous TH lymphocyte trafficking. Blood. 2003;101(5):1677-82.
E16. Homey B, Alenius H, Muller A, Soto H, Bowman EP, Yuan W, et al. CCL27-CCR10 interactions regulate T cell-mediated skin inflammation. Nat Med. 2002;8(2):157-65.
E17. Salimi M, Barlow JL, Saunders SP, Xue L, Gutowska-Owsiak D, Wang X, et al. A role for IL-25 and IL-33-driven type-2 innate lymphoid cells in atopic dermatitis. J Exp Med. 2013;210(13):2939-50.
E18. Bernink JH, Ohne Y, Teunissen MBM, Wang J, Wu J, Krabbendam L, et al. c-Kit-positive ILC2s exhibit an ILC3-like signature that may contribute to IL-17-mediated pathologies. Nat Immunol. 2019;20(8):992-1003.
E19. Kimple ME, Neuman JC, Linnemann AK, Casey PJ. Inhibitory G proteins and their receptors: emerging therapeutic targets for obesity and diabetes. Exp Mol Med. 2014;46:e102.
E20. Duchene J, Schanstra JP, Pecher C, Pizard A, Susini C, Esteve JP, et al. A novel protein-protein interaction between a G protein-coupled receptor and the phosphatase SHP-2 is involved in bradykinin-induced inhibition of cell proliferation. J Biol Chem. 2002;277(43):40375-83.
E21. Stockenhuber K, Hegazy AN, West NR, Ilott NE, Stockenhuber A, Bullers SJ, et al. Foxp3(+) T reg cells control psoriasiform inflammation by restraining an IFN-I-driven CD8(+) T cell response. J Exp Med. 2018;215(8):1987-98.
E22. Swindell WR, Michaels KA, Sutter AJ, Diaconu D, Fritz Y, Xing X, et al. Imiquimod has strain-dependent effects in mice and does not uniquely model human psoriasis. Genome Med. 2017;9(1):24.

Supplemental Figure Legends

Figure E1. (**A**) Representative pictures of untreated and 5 day-IMQ-treated skin of $CCR10^{-/-}$ and $CCR10^{+/-}$ mice. (**B**) Flow cytometric analysis of gated γδT cells of untreated and IMQ-treated skin of $CCR10^{+/-}$ and $CCR10^{-/-}$ mice for their expression of EGFP (CCR10). The bar graphs on the right show average mean fluorescent intensities (MFI) of EGFP(CCR10) signals of γδT cells in the untreated and IMQ-treated skin of $CCR10^{+/-}$ and $CCR10^{-/-}$ mice. N=5.

Figure E2. (**A**) Flow cytometric analysis of the IL-17A and IL-22 expression by gated αβT cells of the untreated and 5 day-IMQ-treated skin of $CCR10^{-/-}$ and $CCR10^{+/-}$ mice. (**B-C**) Average percentages (B) and numbers (C) of $IL\text{-}17A^{+}$ αβT cells and $IL\text{-}17A^{+}IL\text{-}22^{+}$ αβT cells of the untreated and 5 day-IMQ-treated skin of $CCR10^{-/-}$ and $CCR10^{+/-}$ mice. N=5-6.

Figure E3. (**A**) Flow cytometric analysis of gated αβT cells of untreated and IMQ-treated skin of $CCR10^{+/-}$ and $CCR10^{-/-}$ mice for their expression of EGFP (CCR10). The bar graphs on the right show average percentages of αβT cells that express EGFP(CCR10) in the untreated and IMQ-treated skin of $CCR10^{+/-}$ and $CCR10^{-/-}$ mice. N=5-6. (**B**) Flow cytometric analysis of gated $IL\text{-}17A^{+}IL\text{-}22^{+}$, $IL\text{-}17A^{+}IL\text{-}22^{-}$, and $IL\text{-}17A^{-}IL\text{-}22^{-}$ αβT cells of IMQ-treated skin of $CCR10^{+/-}$ and $CCR10^{-/-}$ mice for their expression of EGFP (CCR10).

Figure E4. (A) Flow cytometric analysis of gated $CD45^{+}$ lymphocytes for $CD3^{-}Lin^{-}$ ILCs (left) and average percentages of ILCs (right) of the untreated and 5 day-IMQ-treated skin of $CCR10^{+/-}$ and $CCR10^{-/-}$ mice. N= 5-6. (**B**) Flow cytometric analysis of gated $CD45^{+}Lin^{-}CD3^{-}$ ILCs for their expression of IL-17A and IL-22 (left) and average percentages of $IL\text{-}17A^{+}$ ILCs (right) of the untreated and 5 day-IMQ-treated skin of $CCR10^{+/-}$ and $CCR10^{-/-}$ mice. N=5-6. Note that there were no $IL\text{-}22^{+}$ ILCs. (**C**) Flow cytometric analysis of gated $CD45^{+}Lin^{-}CD3^{-}$ ILCs for their EGFP(CCR10) expression (left) and average percentages of $EGFP(CCR10)^{+}$ ILCs (right) in the untreated and 5 day-IMQ-treated skin of $CCR10^{+/-}$ and $CCR10^{-/-}$ mice. N=5-6.

Figure E5. (A) H&E-stained sections of the IMQ-treated skin of $Rag1^{-/-}$ mice reconstituted with $CCR10^{+/-}$ or $CCR10^{-/-}$ $CD4^{+}$ T cells. (**B**) Flow cytometric analysis of the EGFP (CCR10) expression on gated $IL\text{-}17A^{+}IL\text{-}22^{+}$, $IL\text{-}17A^{+}IL\text{-}22^{-}$ and $IL\text{-}17A^{-}IL\text{-}22^{-}$ αβT cells of IMQ-treated skin of $Rag1^{-/-}$ mice reconstituted with $CCR10^{+/-}$ or $CCR10^{-/-}$ $CD4^{+}$ αβT cells.

Figure E6. H&E-stained sections of the IMQ-treated skin of $CCR10^{+/-}Rag1^{-/-}$ or $CCR10^{-/-}Rag1^{-/-}$ mice reconstituted with same $CCR10^{+/-}$ $CD4^{+}$ T cells.

Figure E7. (A) Confocal microscopic image of a focused area (30μm depth from the surface) of the skin injected with arrays of microneedles carrying DyLight 650-labeled protein (Red). **(B)** Fluorescent microscopic image of skin sections for visualization of microneedle-mediated protein delivery (Red). Counter-stained with DAPI. **(C)** Images of the IMQ-applied skin treated with a CCL27-loaded or empty (control) microneedle patch. Red boxes: microneedle-treated areas. Mice were topically applied with IMQ daily and treated with microneedles on day 0 and 3. Note that the CCL27-treated area has obvious reduced inflammation on Day 4. **(D)** No significant difference in numbers of αβT cells, percentages and numbers of ILCs in the CCL27 and control microneedle-treated skin. One dot represents one sample.

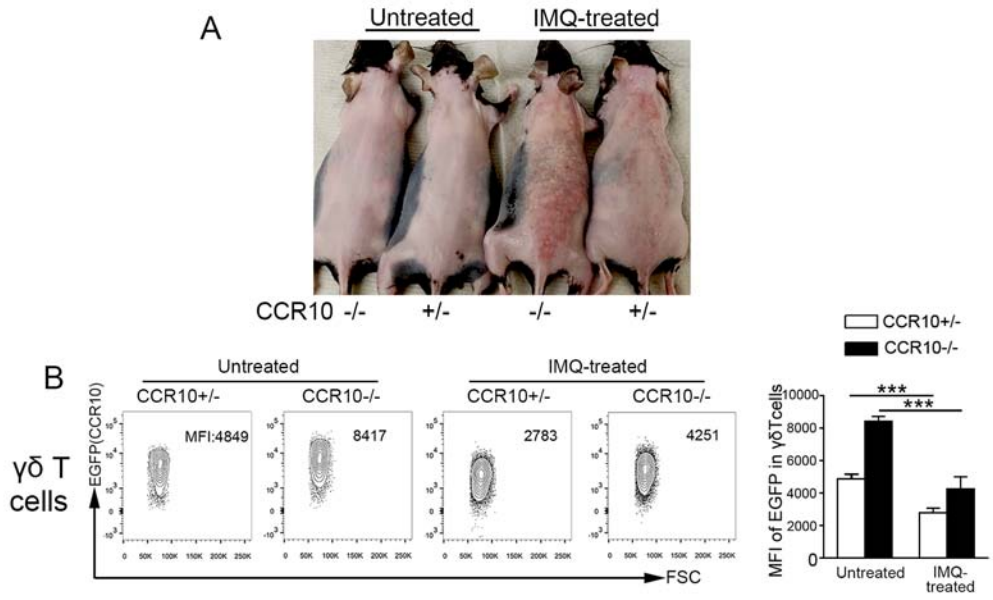

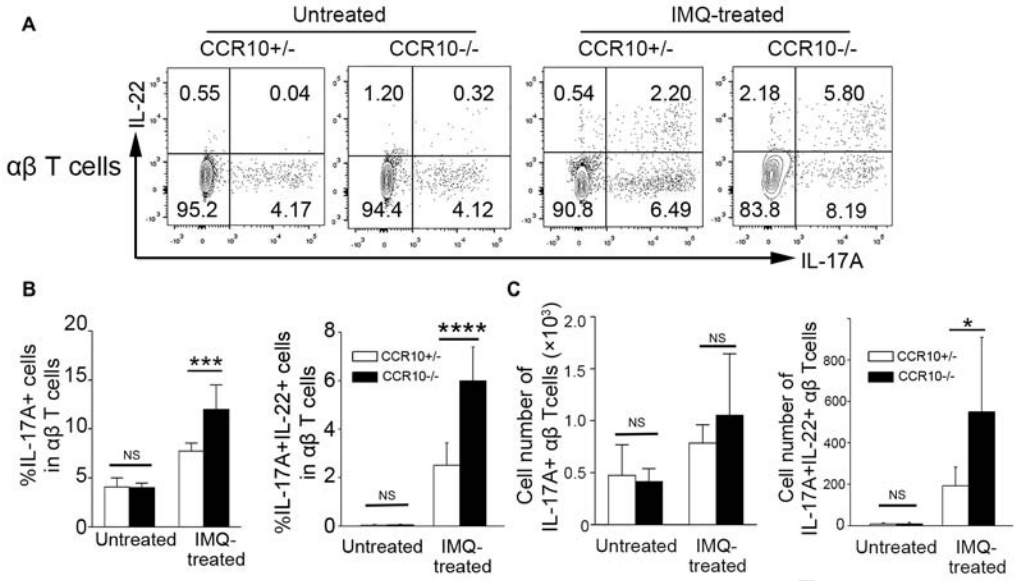

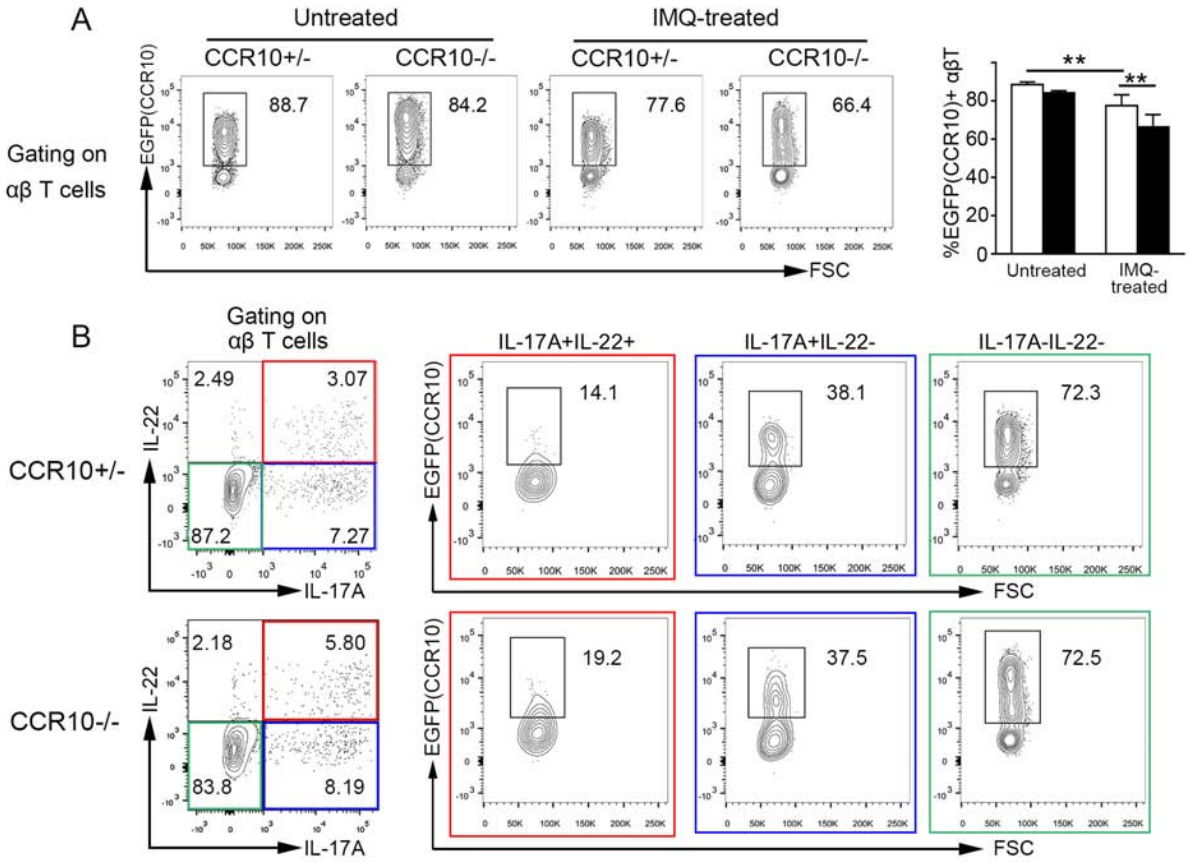
A
Untreated
IMQ-treated
CCR10+/-
CCR10-/-
CCR10+/-
CCR10-/-
Gating on
αβ T cells
EGFP(CCR10)
88.7
84.2
77.6
66.4
FSC
%EGFP(CCR10)+ αβT
**
**
Untreated
IMQ-
treated
B
Gating on
αβ T cells
IL-17A+IL-22+
IL-17A+IL-22-
IL-17A-IL-22-
CCR10+/-
CCR10-/-
IL-22
IL-17A
2.49
3.07
87.2
7.27
2.18
5.80
83.8
8.19
EGFP(CCR10)
14.1
38.1
72.3
19.2
37.5
72.5
FSC

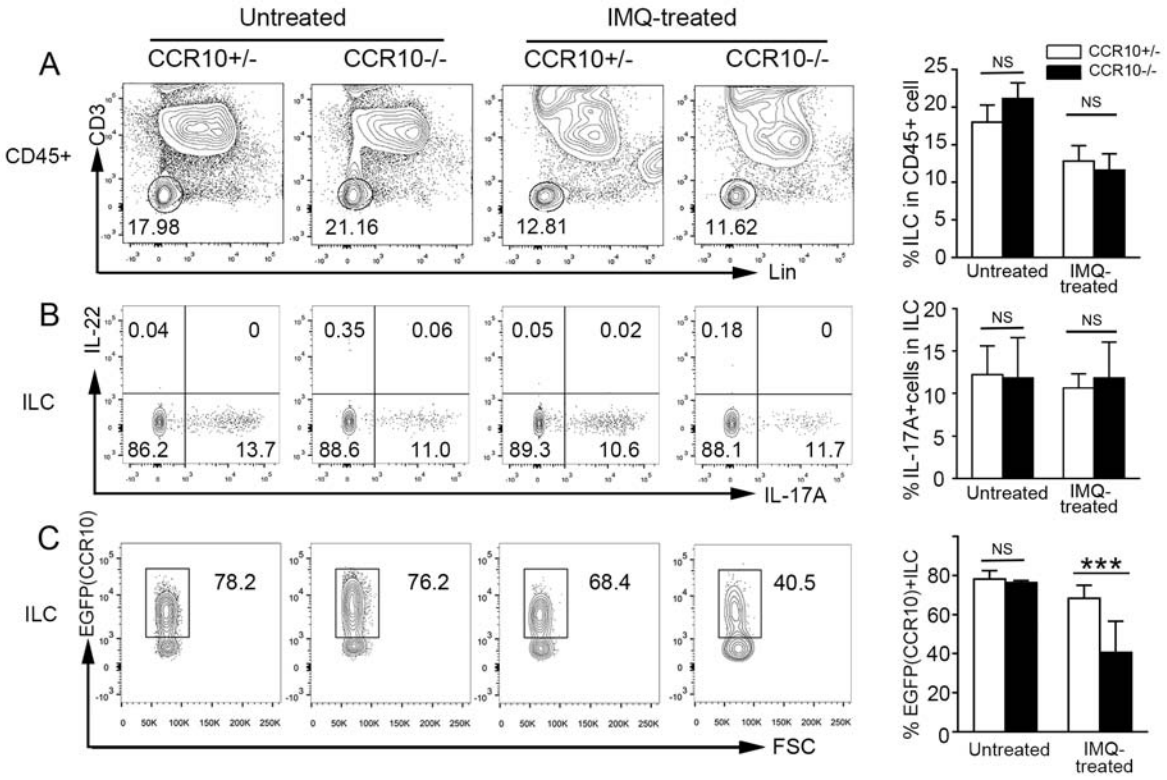
Untreated
IMQ-treated
A
CCR10+/-
CCR10-/-
CCR10+/-
CCR10-/-
CD45+
CD3
17.98
21.16
12.81
11.62
Lin
B
IL-22
ILC
0.04
0
0.35
0.06
0.05
0.02
0.18
0
86.2
13.7
88.6
11.0
89.3
10.6
88.1
11.7
IL-17A
C
ILC
EGFP(CCR10)
78.2
76.2
68.4
40.5
FSC
CCR10+/-
CCR10-/-
NS
NS
% ILC in CD45+ cell
Untreated
IMQ-treated
NS
NS
% IL-17A+cells in ILC
Untreated
IMQ-treated
NS
***
% EGFP(CCR10)+ILC
Untreated
IMQ-treated

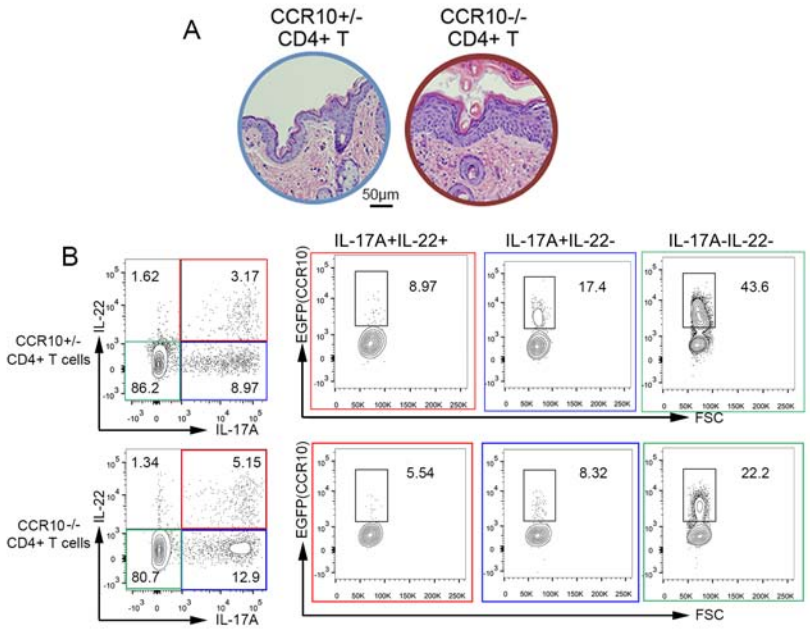

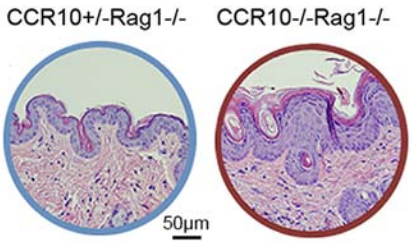

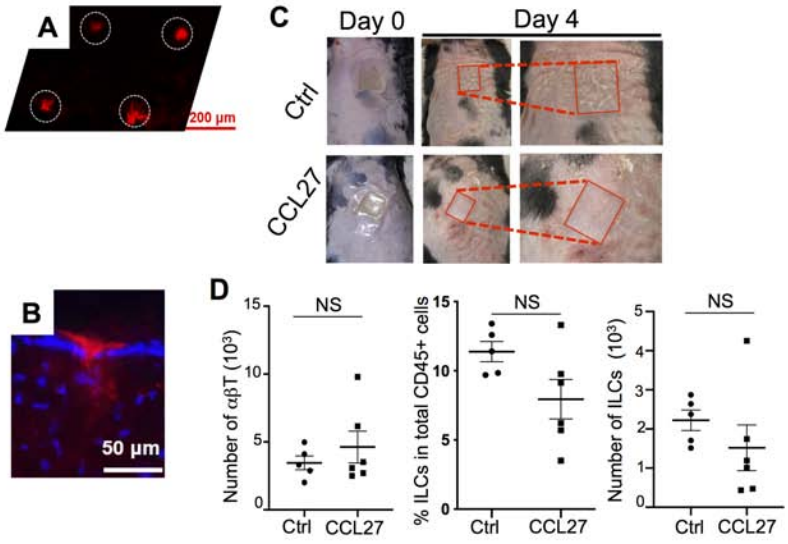
A
200 µm
B
50 µm
C
Day 0
Day 4
Ctrl
CCL27
D
NS
Number of αβT (10³)
Ctrl
CCL27
NS
% ILCs in total CD45+ cells
Ctrl
CCL27
NS
Number of ILCs (10³)
Ctrl
CCL27